Journal of Crystal Growth 312 (2010) 1199–1204

Contents lists available at ScienceDirect

Journal of Crystal Growth

journal homepage: www.elsevier.com/locate/jcrysgro

GaN-cored heteronanowires sheathed with Pt shells: Preparation and annealing studies

Ju Chan Yang, Han Gil Na, Mesfin Abayneh Kebede, Hyo Sung Kim, Hyoun Woo Kim *

Division of Materials Science and Engineering, Inha University, Incheon 402-751, Republic of Korea

ARTICLE INFO

Available online 4 January 2010

Keywords:
A1. Nanowires
A1. Sputtering
A1. Thermal annealing
B1. GaN
B1. Metals

ABSTRACT

We have prepared GaN-core/Pt-shell composite nanowires via a two-step process. With the crystalline Pt shell layer being deposited with a deposition rate of about 4.5 nm/min, it was agglomerated to become cluster-like structures by the subsequent thermal annealing. The shell layers corresponded mainly to a cubic Pt phase regardless of annealing, whereas PtO_x phases were additionally observed. From Gaussian deconvolution studies, the photoluminescence (PL) spectra were divided into three Gaussian functions, which were centered in the ultraviolet (UV), green, and red region, respectively. The overall PL intensity was increased by increasing the annealing temperature. We have discussed the associated PL mechanisms.

1. Introduction

With a variety of potential applications, including blue and ultraviolet light-emitting diodes and laser diodes, high temperature and high power optoelectronic devices, modulators, detectors, gallium nitride (GaN) nanowires have been the subject of intense studies [1–4]. On the other hand, platinum (Pt) is one of the most important transition metal, being used extensively in semiconductor devices including an electrode material for the capacitor structures in memory devices [5]. Additionally, Pt-based metallization schemes have been employed to obtain reliable ohmic contacts to p-GaN [6] and n-GaN [7]. Furthermore, since hydrogen atoms can diffuse very quickly towards Pt-GaN interface, the combination of GaN with catalytic Pt has been used to realize sensors for hydrogen and hydrocarbon gases [8].

With the nanostructures having exhibited novel size-dependent properties [9], one-dimensional (1D) heterostructures of modulated composition and interfaces are supposed to have diverse functionalities. However, metal/semiconductor nanocables could not be sufficiently studied, due to the difficulty in forming a metal shell layers on core nanowires. In the present work, we have prepared GaN/Pt core–shell heteronanowires by directly sputtering Pt onto GaN core nanowires. The Pt shell layer will not only prevent the degradation of core GaN nanowires but also extend their functionalities. The fabrication of nanodevices inevitably comprises thermal annealing process, which will alter/enhance the properties of core/shell nanowires. Accordingly, we have investigated the effects of thermal annealing on the structural and optical properties of as-fabricated GaN-core/Pt-shell nanowires.

2. Experimental

In the first step, we have prepared core GaN nanowires on silver (Ag: about 10 nm)-coated Si substrates, by heating pure GaN powders in a tube furnace. During the process, Ar (flow rate: 100 sccm) and NH_3 (flow rate: 20 sccm) gases was flowed at 1000 °C for 1 h. In the second step, the substrates were transferred to a turbo sputter coater (Emitech K575X, Emitech Ltd., Ashford, Kent, UK) [10]. With using a circular Pt target at room temperature, the DC current was maintained at 30 mA. Subsequently, in order to investigate the effects of thermal annealing, we have heated the GaN-core/Pt-shell nanowires at temperatures in the range 500–900 °C, for 30 min in N_2 ambient.

The product was characterized by scanning electron microscopy (SEM, Hitachi, S-4200) and transmission electron microscopy (TEM, Philips CM-200). X-ray powder diffraction (XRD) was performed by using a Philips X'pert MRD diffractometer. A He–Cd laser (55 mW, wavelength at 325 nm) was employed to measure the photoluminescence (PL) of the sample.

3. Results and discussion

Figs. 1a–d show the SEM-based diameter distributions of the uncoated GaN nanowires (sample A), the GaN/Pt core/shell

* Corresponding author. Tel.: +82 32 860 7544; fax: +82 32 862 5546.
E-mail address: hwkim@inha.ac.kr (H.W. Kim).

0022-0248/$ - see front matter © 2009 Elsevier B.V. All rights reserved.
doi:10.1016/j.jcrysgro.2009.12.049

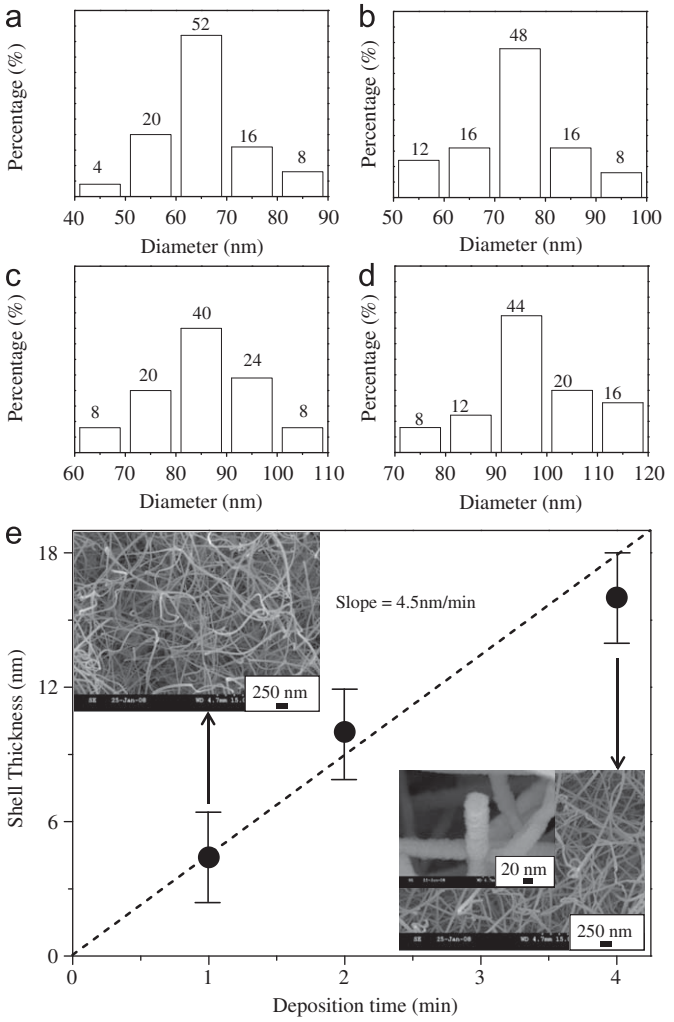

Fig. 1. SEM-based diameter distributions of (a) uncoated GaN nanowires and GaN-core/Pt-shell nanowires sputtered with (b) 1 min, (c) 2 min, and (d) 4 min. (e) Dependence of the average thickness of shell layers on deposition time.

nanowires with a sputter time of 1 (sample B), 2 (sample C), and 4 (sample D). Accordingly, the average diameter of samples A, B, C, and D, is calculated to be 65.4, 74.2, 85.4, and 97.4 nm, respectively. It is thereupon estimated that the average shell thicknesses (per side) of 1-, 2-, and 4-min-sputtered nanowires are approximately 4.4, 10, and 16.0 nm, respectively. The shell thickness tends to increase almost linearly with the growth time, as shown in Fig. 1e. The deposition rate of the Pt coating is determined in a straightforward manner from the plot to be about 4.5 nm/min. Magnified SEM image of the 4-min-sputtered sample exhibited the rough surface, revealing that the present sputtering is not a uniform process.

Fig. 2a shows a low-magnification TEM image of a GaN/Pt core/shell nanowire, clearly indicating that there are two segments in the structure: a rod-like core and thin coating layers (on both sides). The outer solid layer, which was formed by the second step, is relatively smooth and continuous along the nanowire. Fig. 2b shows a corresponding SAED pattern, exhibiting diffraction rings of Pt. An enlarged TEM image as shown in Fig. 2c reveals that the shell is crystalline, in which the spacings between lattice planes are about 0.22 and 0.19 nm, corresponding to spacing d_{111} and d_{200} of cubic Pt.

Fig. 3a shows a SEM image of GaN-core/Pt-shell nanowires annealed at 700 °C. Although close examination revealed that the nanowire surface became rougher by the thermal annealing, it is apparent that the annealed structures maintain their 1D morphology. The inset of Fig. 3a reveals that the 900 °C-annealed sample has a noticeably rough surface. Fig. 3b shows a low-magnification TEM image of a GaN-core/Pt-shell nanowire annealed at 700 °C, exhibiting the blackened cluster-like regions. Figs. 3c and d show the associated elemental maps of Ga and Pt, respectively. The Pt atoms have been concentrated in the blackened part of Fig. 3b, suggesting that the cluster-like structures in Fig. 3b comprised Pt elements. Fig. 3e shows the associated SAED pattern, confirming the existence of diffraction rings of cubic Pt. It is noteworthy that shell layers mainly comprise a cubic Pt phase in spite of thermal annealing.

Fig. 4a shows an XRD pattern of uncoated GaN nanowires, indicating that the whole spectrum can be indexed to a crystalline hexagonal wurtzite GaN phase (JCPDS card: No. 50-0792). Fig. 4b shows an XRD spectrum of GaN/Pt core–shell nanowires, revealing that there exists a cubic Pt phase (JCPDS card: No. 04-0802), in addition to the GaN phase. Figs. 4c and d represent XRD spectra of 500- and 900 °C-annealed GaN/Pt core–shell nanowires, respectively. Fig. 4c clearly exhibits the Pt-related diffraction peaks. By comparing Fig. 4d with Fig. 4c, we reveal that the relative intensity of Pt- to GaN-associated peaks increased with increasing the annealing temperature from 500 to 900 °C. Furthermore, there exist very weak diffraction peaks in regard to the Pt_3O_4 and PtO_2 phases, indicating that a trace amount of Pt_3O_4 and PtO_2 phases has been generated by the thermal annealing.

Fig. 5a shows a PL spectrum of Pt-coated GaN nanowires, which was subsequently annealed at 500 °C. The spectrum is nearly identical to those of GaN core nanowires and as-synthesized Pt-coated GaN nanowires, indicating that the Pt coating and subsequent thermal annealing at 500 °C did not significantly alter the optical properties. The broad emission can be divided into three Gaussian functions, which were centered at 3.2 eV in the ultraviolet (UV) region, 2.4 eV in the green region, and 1.9 eV in the red region, respectively. Fig. 5b shows a PL spectrum of 900 °C-annealed GaN-core/Pt-shell nanowires. Being similar to 500 °C-annealed sample, the PL spectrum exhibited three peaks, centered at 1.9, 2.3, and 3.2 eV, respectively. The intensities of red, green, ultraviolet (UV) emission peaks have been increased by the thermal annealing.

It is known that the UV band in GaN is attributed to the transition from a shallow donor to a shallow acceptor [11]. Main candidates for the shallow donors are Si_{Ga} and O_N, whereas those for the shallow acceptors are Si_N and C_N [11]. Also, the green emission is ascribed to structural defects, including V_{Ga}, V_{Ga}–O_N complexes, etc. [11,12]. On the other hand, red emission band in GaN is generally ascribed to vacancy-impurity pairs [13–15], such as a deep donor V_NC_N and a deep acceptor $V_{Ga}O_N$ [16,17]. It is surmised that the diffusion of Si from the substrate and C and O from inside the chamber will be activated by the thermal annealing at a sufficiently high temperature, ultimately enhancing the UV and red emission. The thermal annealing will also favor the generation of vacancy-related structural defects, enhancing the green emission. Also, Pt was found to be a fast diffuser, becoming a shallow donor in GaN [18]. The formation of Ga vacancies can be enhanced by complex formation with donor (Pt) impurity, presumably contributing to the enhancement of green emission [18]. The other possibility is that the generated PtO_x compounds affected the emission. For example, it has been reported that Pt^{4+} in octahedral complexes exhibited a red emission [19]. In addition, it is noteworthy that the ratio of the intensity of red emission to that of UV

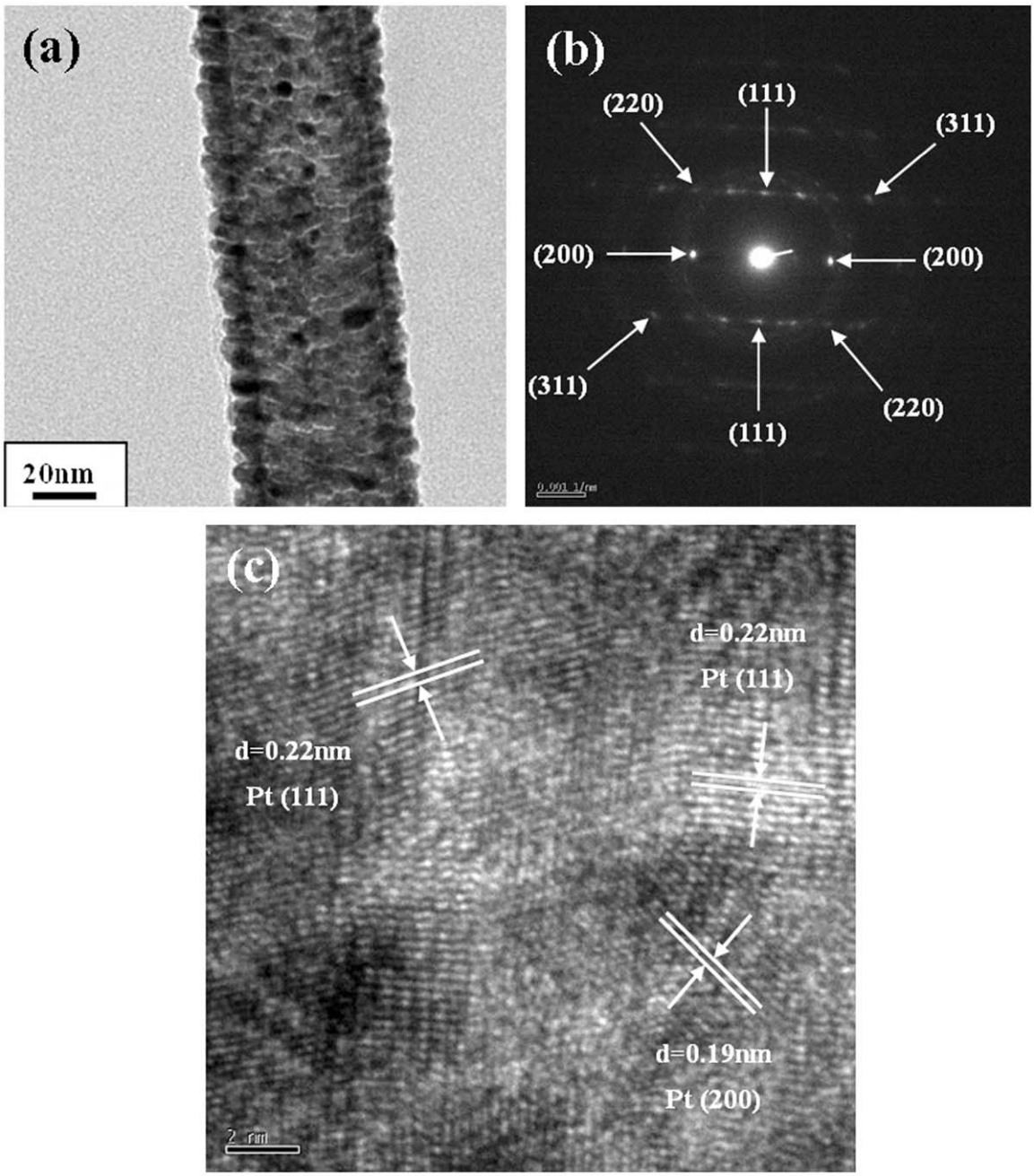

Fig. 2. (a) TEM image of an as-synthesized GaN-core/Pt-shell nanowire. (b) Associated SAED pattern image. (c) Lattice-resolved TEM image enlarging an area near the surface of the nanowires in (a).

emission has been increased with increasing the annealing temperature. From the above discussion, we realize that the UV emission is associated with Si_{Ga}, O_N, Si_N, and C_N, whereas the red emission is related to V_NC_N and $V_{Ga}O_N$. We surmise that the activation energy of Si diffusion is relatively higher than those of diffusion of vacancy, O, and C, resulting in the observed phenomenon.

4. Conclusions

We have fabricated GaN-core/Pt-shell nanowires. The Pt shell thickness tends to increase almost linearly with the sputter time, with a growth rate of about 4.5 nm/min. By thermal annealing the Pt shell layers, not only morphological changes but also the generation of a trace amount of PtO_x phases has been observed. PL analysis with Gaussian deconvolution indicates that the PL spectra consist of three major emission bands, which were centered at 1.9, 2.4, and 3.2 eV, respectively. Although subsequent thermal annealing did not significantly change the peak positions of those emission bands, it enhanced their intensity. It is possible that the annealing-induced change in PL spectra resulted not only from the impurity and vacancy-related defects in GaN, but also from PtO_x compounds.

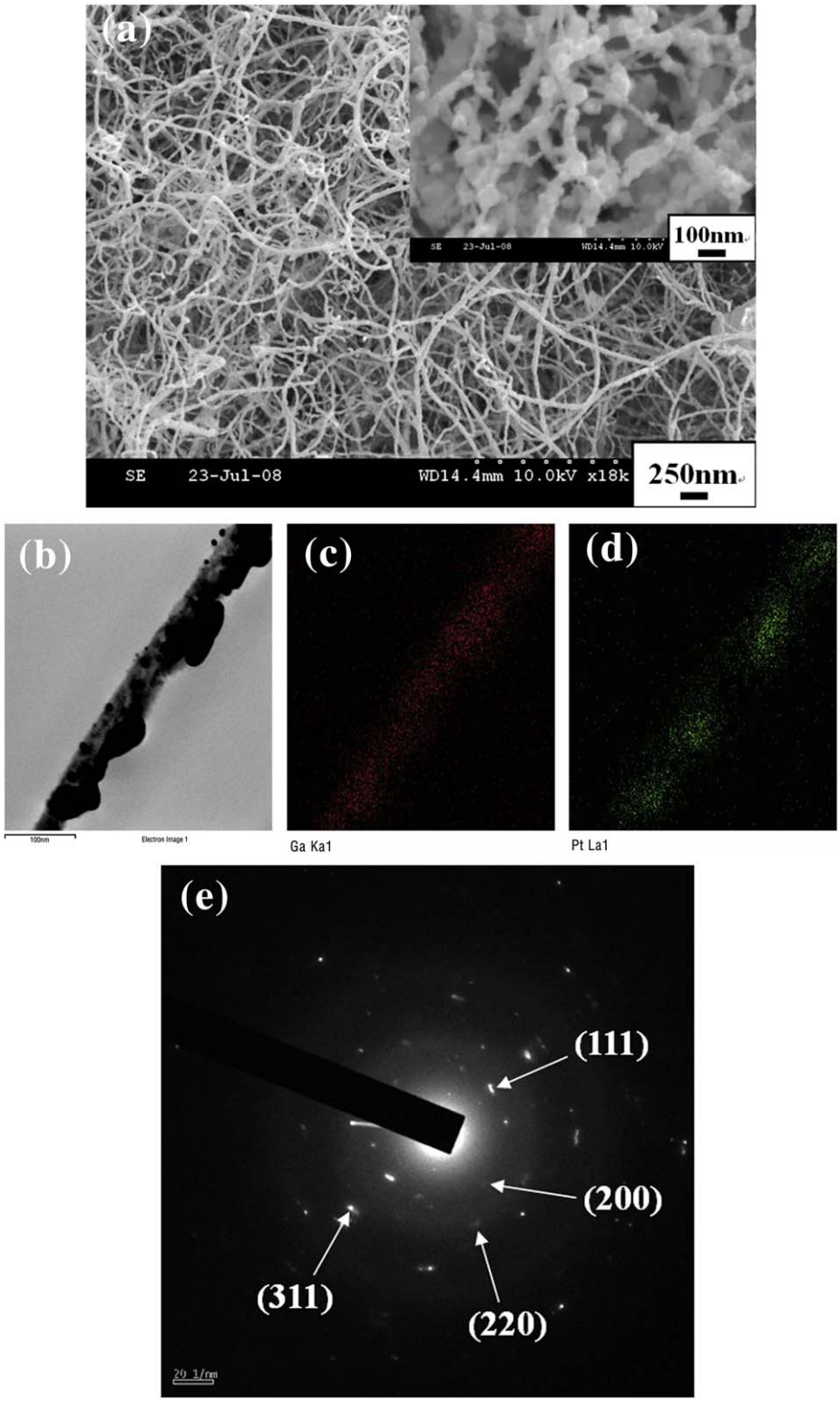

Fig. 3. (a) SEM image of GaN-core/Pt-shell nanowires annealed at 700 °C (inset: SEM image of GaN-core/Pt-shell nanowires annealed at 900 °C). (b) TEM image of a GaN-core/Pt-shell nanowires annealed at 700 °C and associated elemental maps of (c) Ga elements and (d) Pt elements. (e) Corresponding SAED pattern image.

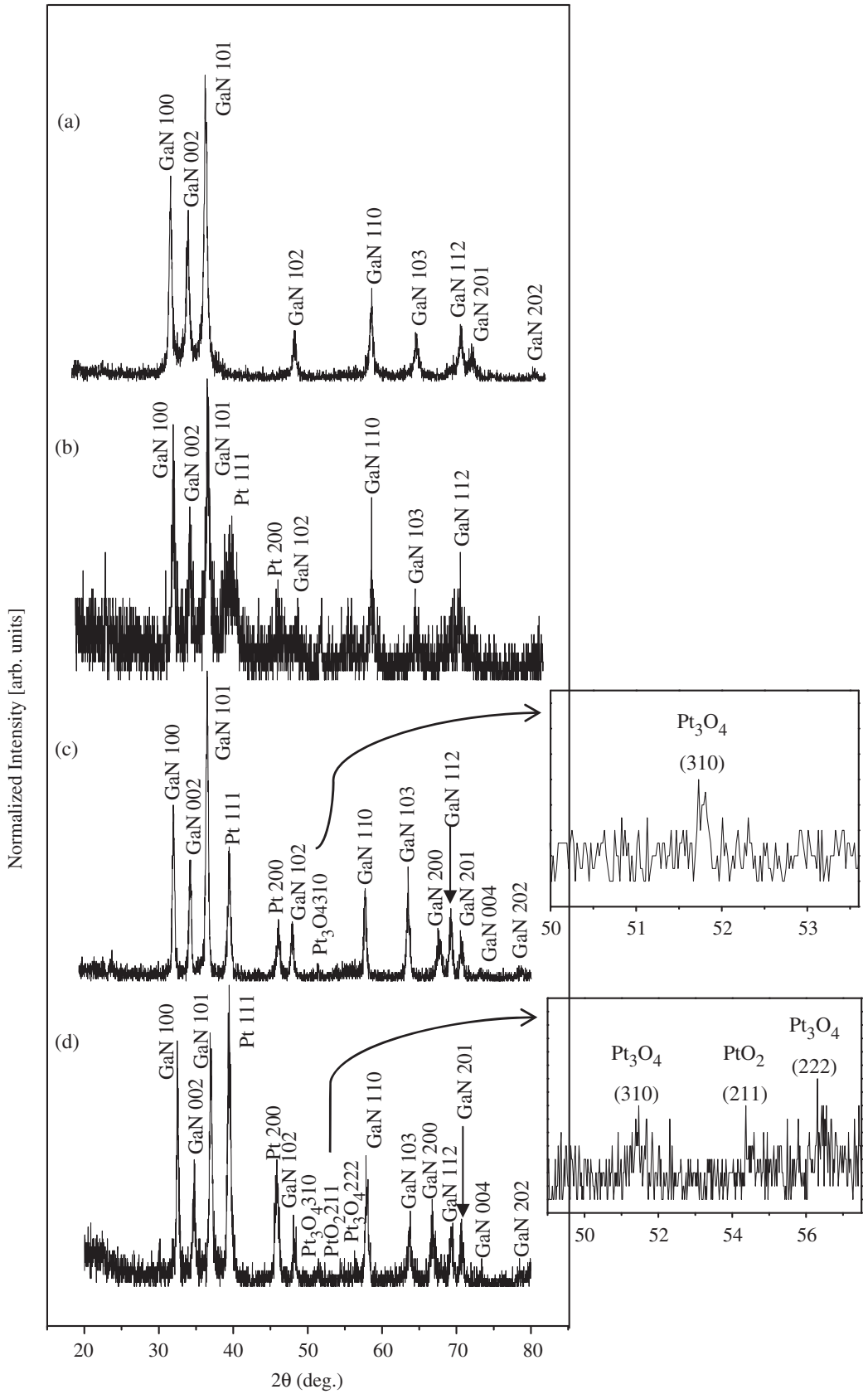

Fig. 4. XRD patterns of (a) uncoated GaN nanowires, (b) unannealed, (c) 500 °C-annealed, and (d) 900 °C-annealed GaN-core/Pt-shell nanowires.

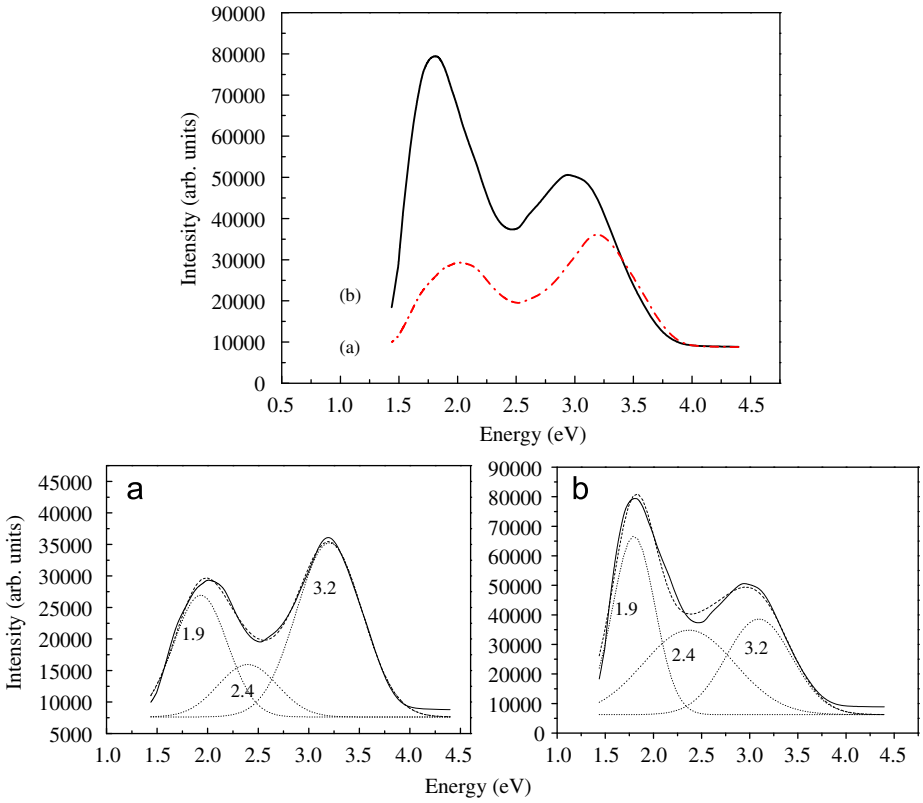

Fig. 5. PL spectra of GaN-core/Pt-shell nanowires annealed at (a) 500 °C and (b) 900 °C.

Acknowledgements

This work was supported by a Korea Research Foundation Grant funded by the Korean Government (MOEHRD) (KRF-2007-521-D00216). The main calculations were performed by the supercomputing resources of the Korea Institute of Science and Technology Information (KISTI).

References

[1] J. Zolper, R. Shul, A. Baca, R. Wilson, S. Pearton, R. Stall, Appl. Phys. Lett. 68 (1996) 2273.
[2] B. Liu, Y. Bando, C. Tang, F. Xu, J. Hu, D. Golberg, J. Phys. Chem. B 109 (2005) 17082.
[3] H.M. Kim, Y.H. Choo, H. Lee, S.I. Kim, S.R. Ryu, D.Y. Kim, T.W. Kang, K.S. Chung, Nano Lett. 4 (2004) 1059.
[4] Y. Huang, X. Duan, Y. Cui, C.M. Lieber, Nano Lett. 2 (2002) 101.
[5] H.-W. Kim, B.-S. Ju, B.-Y. Nam, W.-J. Yoo, C.-J. Kang, T.-H. Ahn, J.-T. Moon, M.-Y. Lee, J. Vac. Sci. Technol. A 17 (1999) 2151.
[6] J.-S. Jang, S.-J. Park, T.-Y. Seong, J. Electrochem. Soc. 146 (1999) 3425.
[7] C.Y. Hu, Z.B. Ding, Z.X. Qin, Z.Z. Chen, Y.J. Wang, Z.J. Yang, X.D. Hu, T.J. Yu, L.S. Yu, S.D. Yao, G.Y. Zhang, Semicond. Sci. Technol. 21 (2006) 938.
[8] M. Ali, V. Cimalla, V. Lebedev, H. Romanus, V. Tilak, D. Merfeld, P. Sandvik, O. Ambacher, Sens. Actuators B 113 (2006) 797.
[9] J.P. Wilcoxon, J.E. Martin, F. Parsapour, B. Wiedenman, D.F. Kelley, J. Chem. Phys. 108 (1998) 9137.
[10] H.W. Kim, S.H. Shim, J.W. Lee, Carbon 45 (2007) 2695.
[11] M.A. Reshchikov, H. Morkoç, J. Appl. Phys. 97 (2005) 061301.
[12] M.A. Reshchikov, H. Morkoc, S.S. Park, K.Y. Lee, Appl. Phys Lett. 78 (2001) 3041.
[13] S. Nakamura, N. Iwasa, M. Senoh, T. Mukai, Jpn. J. Appl. Phys. 31 (1992) 1258.
[14] U. Kaufmann, M. Kunzer, H. Obloh, M. Maier, Ch. Manz, A. Ramakrishnan, B. Santic, Phys. Rev. B 59 (1999) 5561.
[15] D.M. Hofmann, B.K. Meyer, H. Alves, F. Leiter, W. Burkhard, N. Romanov, Y. Kim, J. Krüger, E.R. Weber, Phys. Status Solidi (a) 180 (2000) 261.
[16] L. Wang, E. Richter, M. Weyers, Phys. Status Solidi (a) 204 (2007) 846.
[17] S. Zeng, G.N. Aliev, D. Wolverson, J.J. Davies, S.J. Bingham, D.A. Abdulmalik, P.G. Coleman, T. Wang, P.J. Parbrook, Phys. Status Solidi (c) 3 (2006) 1919.
[18] L.-Z. Hsieh, D.-H. Yeh, J. Appl. Phys. 102 (2007) 024607.
[19] I.N. Douglas, J.V. Nicholas, B.G. Wybourne, J. Chem. Phys. 48 (1968) 1415.